

Published in final edited form as:

Ann Surg. 2009 February ; 249(2): 277–285. doi:10.1097/SLA.0b013e3181904af0.

## Mechanisms of Glucose Homeostasis After Roux-en-Y Gastric Bypass Surgery in the Obese, Insulin-Resistant Zucker Rat

Katia Meirelles, MD<sup>\*</sup>, Tamer Ahmed, MD<sup>\*</sup>, Derek M. Culnan, MD<sup>\*</sup>, Christopher J. Lynch, PhD<sup>†</sup>, Charles H. Lang, PhD<sup>\*,†</sup>, and Robert N. Cooney, MD<sup>\*,†</sup>

<sup>\*</sup> Department of Surgery, Pennsylvania State University College of Medicine, Hershey, PA

<sup>†</sup> Department of Cellular and Molecular Physiology, Pennsylvania State University College of Medicine, Hershey, PA

### Abstract

**Objective**—Obesity-related diabetes is caused by insulin resistance and  $\beta$ -cell dysfunction. The current study examines changes in food intake, weight loss, body fat depots, oxygen consumption, insulin sensitivity, and incretin levels as potential mechanisms for improved glucose tolerance after Roux-en-Y gastric bypass (RYGB).

**Methods**—Three groups of genetically obese Zucker rats were studied: RYGB, sham surgery paired (PF), and sham surgery ad libitum (AL) fed rats. Changes in body weight, visceral and subcutaneous fat depots, oral glucose tolerance, insulin sensitivity, and the plasma concentrations of insulin, glucagon, glucagon-like peptide-1 (GLP-1), glucose-dependent insulinotropic peptide, and peptide YY (PYY) were measured.

**Results**—Body weight and subcutaneous fat were decreased after RYGB, compared with the PF and AL groups. The reduction in visceral fat after RYGB appeared largely because of food restriction. Glucose tolerance and insulin sensitivity were significantly improved in only the RYGB group ( $P < 0.05$  vs. AL, PF). Euglycemic, hyperinsulinemic clamp studies indicated RYGB improved the ability of insulin to stimulate peripheral (eg, skeletal muscle) glucose uptake. Fasting total GLP-1, glucose-dependent insulinotropic peptide, and PYY levels were similar between the groups, whereas postprandial plasma levels of intact GLP-1 (7–36) amide, total GLP-1, and PYY were increased in the RYGB group compared with PF and AL controls.

**Conclusions**—Glucose homeostasis after RYGB is associated with decreased subcutaneous fat, increased postprandial PYY, GLP-1, and insulin, as well as improved insulin sensitivity/action. Changes in food intake and visceral fat do not seem to explain improvements in insulin action after RYGB in the Zucker rat model.

### Keywords

gastric bypass; obesity; diabetes; incretin; GLP-1

---

Obesity is a leading cause of morbidity and mortality worldwide. Morbid obesity, its most severe form, afflicts 23 million Americans.<sup>1</sup> Surgery is currently the most effective treatment for morbid obesity.<sup>2</sup> The Roux-en-Y gastric bypass (RYGB) is the most common bariatric procedure performed in the United States. The RYGB produces durable weight loss and

---

Reprints: Robert N. Cooney, MD, Department of Surgery, Pennsylvania State University, College of Medicine, Hershey, PA 17033. E-mail: rcooney@hmc.psu.edu.

The Department specifically disclaims responsibility for any analyses, interpretations or conclusions.

significant improvements in obesity-related medical conditions including: hypertension, hyperlipidemia, sleep apnea, arthritis, infertility, and type 2 diabetes mellitus (T2DM).<sup>2-5</sup> Many patients demonstrate significant improvements in T2DM shortly after RYGB surgery, before significant weight loss.<sup>6,7</sup> This observation has raised questions regarding the relative importance of decreased food intake, weight loss, changes in fat depots, and/or bypass of the hormonally active foregut in improving obesity-related insulin resistance.<sup>8</sup> The current study examines potential mechanisms for early postoperative glucose homeostasis after RYGB using the genetically obese Zucker rat model.

Obesity in the Zucker rat is an autosomal recessive trait (fa/fa) caused by defective leptin receptors.<sup>9,10</sup> Heterozygous lean Zucker rats are normal, whereas the obese Zucker rat develops progressive insulin resistance, glucose intolerance, hyperlipidemia, and hypertension.<sup>11</sup> The obese Zucker rat has been used extensively to study obesity-related insulin resistance and is therefore an excellent model for investigating how RYGB improves glucose homeostasis.<sup>12</sup> In the obese Zucker rat, peripheral insulin resistance is characterized by moderately elevated circulating glucose levels, hyperinsulinemia, abnormal glucose tolerance, and increased pancreatic  $\beta$ -cell mass.<sup>11</sup> Peripheral insulin resistance in this model is because of defective insulin signaling, reductions in the insulin-sensitive glucose transporter (GLUT4) expression and insulin-stimulated GLUT4 membrane translocation.<sup>13,14</sup>

Early improvements in glucose homeostasis after RYGB may be because of decreased food intake, weight loss, or changes in body composition. Alterations in the secretion or activity of enteric (incretin) or adipose (adipokine) hormones have also been implicated in the resolution of T2DM after RYGB surgery.<sup>15,16</sup> Incretins are peptides secreted by the gut which augment insulin secretion and glycemic control in response to oral (vs. intravenous) glucose, and fat intake.<sup>15</sup> Glucose-dependent insulinotropic peptide (GIP) is secreted by K cells in the duodenum and jejunum whereas glucagon-like peptide-1 (GLP-1) is secreted by L cells in the distal small bowel.<sup>15</sup> Both GIP and GLP-1 bind specific receptors on pancreatic  $\beta$ -cells to increase islet cell mass and stimulate insulin secretion.<sup>15</sup> Extrapankretic effects of GLP-1 include the stimulation of glucose metabolism in liver and muscle.<sup>17,18</sup> GIP levels are not altered in T2DM, but reductions in  $\beta$ -cell GIP receptors and postreceptor defects in GIP signaling have been identified.<sup>19</sup> Impaired GLP-1 release and action have also been identified in T2DM.<sup>20</sup> Thus, alterations in incretin synthesis or activity represent a potential mechanism for improved insulin sensitivity after RYGB surgery.

The quantity and distribution of body fat and the synthesis of adipokines have also been shown to be important in the development of insulin resistance.<sup>21</sup> Accumulation of visceral fat in particular is associated with insulin resistance and removal of visceral fat improves insulin sensitivity and glucose homeostasis.<sup>22</sup> The secretion of adipokines [tumor necrosis factor (TNF $\alpha$ ), interleukin-6 (IL-6), and resistin] by visceral and subcutaneous fat contribute to insulin resistance at the tissue level and are associated with impaired insulin signaling in muscle and other tissues.<sup>23</sup>

The current study was designed to examine the effects of RYGB and pair-feeding on body weight, adipose tissue depots, glucose tolerance, insulin sensitivity, and incretin production. Our data indicate RYGB-induced changes in gastrointestinal anatomy (foregut bypass and enhanced delivery of undigested nutrients to the ileum) result in improved glucose tolerance and insulin action associated with increased GLP-1 concentration.

## MATERIALS AND METHODS

### Animal Care and Surgery

Three groups of male Zucker rats, 10 to 12 weeks of age (Charles River Breeding Laboratories, Wilmington, MA) were studied: RYGB, sham surgery pair-fed (PF) and sham surgery fed ad libitum (AL). Data from 79 rats were included in the study: RYGB (34), PF (23), and AL (22). Body weight data was reported for all animals. The number of animals in each experimental group for different experiments is reported in the figure legend. Animals were housed in wire bottom cages to prevent coprophagia. Except for pretest overnight fasting and the immediate postoperative period, animals had free access to water and chow (Harlan Teklad 2018). The experimental protocols were approved by the Institutional Animal Care and Use Committee at the Pennsylvania State University, College of Medicine.

Before surgery, animals were randomized to the RYGB, PF, or AL groups. The RYGB procedure was performed using a modification of the technique described by Xu et al.<sup>24</sup> The day before surgery rats were made fasted, but provided water. After randomization, rats were weighed, and then anesthetized with isoflurane (3% for induction, 1.5% for maintenance). Ceftriaxone 100 mg/kg intramuscular (Roche, Nutley, NJ) was given as a prophylactic antibiotic. Under sterile conditions a midline laparotomy was performed. Intestinal manipulation was performed in the 2 sham-surgery groups followed by abdominal closure. In the RYGB group, the stomach was divided using a GIA stapler (ETS-Flex Ethicon Endo surgery 45 mm) to create a 20% gastric pouch, the small bowel was divided to create a 15 cm biliopancreatic limb, a 10 cm alimentary (Roux) limb, and a 33 cm common channel. The gastrojejunal and jejunojejunostomies were performed using interrupted 5-0 silk sutures, followed by abdominal closure using 3-0 silk and 5-0 prolene. Surgical incisions were injected with 0.5 mL of 0.25% bupivacaine to minimize postoperative discomfort. All rats were injected subcutaneously with normal saline [50 mL/kg, before the start of surgery, immediately after surgery, and again on postoperative day (POD) 1]. After surgery, animals were housed individually and body weight and food consumption were monitored daily. To allow the surgical anastomoses to heal, animals were not allowed to eat or drink until 24 hours after surgery. Approximately 24 hours after surgery, animals were started on a liquid diet consisting of Resource (Novartis, NY) and access to water AL. Regular chow was started on POD 3, to ensure adequate healing of the stomach and bowel anastomoses. The PF group was given the same amount of food as the RYGB rats consumed and the AL group was allowed to eat AL.

### Oral Glucose Tolerance Tests (OGTT) and Insulin Sensitivity

OGTTs were performed preoperatively and repeated on POD 21. Blood was collected by tail snip before ( $t_0$ ), and 30, 60, 90, and 120 minutes after oral gavage with 1.25 g/kg 25% dextrose in tubes containing 50 mmol/L EDTA, 12 TIU/mL aprotinin, and 100  $\mu$ mol/mL dipeptidyl peptidase-4 inhibitor. Glucose was measured by glucometer (OneTouch Lifescan, Johnson and Johnson, New Brunswick, NJ). Insulin was measured by enzyme-linked immunosorbent assay (ELISA) (ALPCO Diagnostics, Windham, NH) according to the manufacturer's guidelines. Changes in glucose tolerance were compared by analyzing area under the curve (AUC). AUC was calculated using the area under the  $t_0$  starting and  $t_{120}$  ending points for each experimental group. Changes in insulin sensitivity were estimated by mathematical analysis of fasting and postprandial glucose and insulin levels using HOMA ( $G_0 \times I_0 / 22.5$ ), the quantitative insulin sensitivity check (QUICKI)  $1 / [\log(I_0 + \log G_0)]$ , and insulin sensitivity index (ISI)  $10,000 / [\text{fasting plasma glucose (FPG)} \times \text{fasting plasma insulin}] \times \text{mean OGTT glu} \times \text{mean OGTT insulin}$ .<sup>25–28</sup> In the above equations,  $G_0$  and  $I_0$  are the glucose and insulin concentrations before the start of the OGTT.

## Measurement of Visceral and Subcutaneous Fat

Before surgery and on POD 28 after RYGB surgery, magnetic resonance imaging (MRI) was used to quantify visceral and subcutaneous.<sup>29</sup> Animals were sedated using inhalational halothane anesthesia and placed supine within a 15 cm quadrature rf coil. T1 gradient echo images were obtained using a 3T Bruker NMR spectrometer/imager using the following parameters: TR/TE: 350 milliseconds/2.2 milliseconds (in-phase), 4.5 milliseconds (out-of-phase), 10 cm FOV 256 × 256 matrix, and 5 mm section thickness. Total image acquisition time was 1.5 minutes per acquisition. In-plane pixel resolution was 0.39 mm. Duplicate single slice measurements in the L4–L5 region of the spine were taken in 2 sequential studies. Visceral fat areas at this level correlate well with total visceral fat.<sup>30</sup> Manual segmentation of the fat depot images was performed using Adobe Photoshop's (Adobe Systems Incorporated, San Jose, CA) version 7.0 "magic wand" function to generate regions of interest for subcutaneous and intra peritoneal fat areas. Histograms were generated to determine the number of fat-containing pixels in each region of interest. A pooled coefficient of variation (CV%) was calculated from the variation in visceral and subcutaneous measurements using a test/retest protocol. The CV% was 2.5% for subcutaneous and 3.4% for visceral fat, respectively. Preoperative values were normalized to 1 and compared with values from the same rats on POD 28.

## Indirect Calorimetry

Energy expenditure was measured preoperatively and on POD 14 using indirect calorimetry (Oxymax, Columbus Instruments) as previously described.<sup>31</sup> Animals were acclimated in the chamber for 2 hours. Briefly, constant airflow (3.0 L/min) was drawn through the chamber and monitored using a mass-sensitive flow meter. The concentrations of oxygen and carbon dioxide were monitored at the inlet and outlet of the metabolic chambers and used to calculate oxygen consumption ( $\text{VO}_2$ ) and RQ. Each chamber was measured for 1.0 minutes at 15 minutes intervals for 22 hours.

## Hyperinsulinemic, Euglycemic Clamp

On POD 28, Zucker rats were anesthetized using 1% to 3% isoflurane and catheters placed in the jugular vein and carotid artery as previously described.<sup>32</sup> After surgery animals were housed in individual cages, fasted overnight, and provided water AL. The next morning, a primed, constant intravenous infusion of [ $3\text{-}^3\text{H}$ ] glucose (high performance liquid chromatography purified; DuPont-New England Nuclear, Boston, MA) was initiated to determine basal glucose kinetics.<sup>33–35</sup> A 7- $\mu\text{Ci}$  bolus injection of labeled glucose was administered followed by a continuous infusion at a rate of 0.083  $\mu\text{Ci}/\text{min}$  for 2 hours. Arterial blood samples (0.3 mL each) were collected at 100 and 120 minutes after the start of the tracer infusion. Blood was collected in heparinized syringes, centrifuged, and the plasma glucose concentration and glucose specific activity were determined on each sample. Then, regular human insulin (Eli Lilly, Indianapolis, IN) was infused at a rate of 100  $\text{mU} \cdot \text{min}^{-1} \cdot \text{kg}^{-1}$  for 3 hours. This infusion rate results in steady-state plasma insulin concentrations of  $\sim 5000 \mu\text{U}/\text{mL}$ .<sup>33–35</sup> This insulin concentration was used because it maximally stimulates glucose disposal by the whole body and skeletal muscle regardless of fiber type in both normal and insulin-resistant conditions. Titrated glucose was not infused during the clamp because earlier studies indicated this insulin infusion rate completely suppressed endogenous hepatic glucose production in control and obese animals (data not shown). Arterial plasma glucose was measured every 10 to 15 minutes using a glucose analyzer (Analox) and an infusion of 30% D-glucose was used to maintain euglycemia ( $\sim 100 \text{mg}/\text{dL}$ ) during the clamp. The plasma glucose and glucose infusion rate were determined over time. Because the prevailing insulin levels during the hyperinsulinemic clamp completely suppress endogenous glucose production, the rate of whole body glucose disposal equals the exogenous glucose infusion

rate. The increment in insulin-stimulated glucose uptake for each animal was calculated by subtracting the basal endogenous rate of glucose disappearance from the measured rate of glucose disposal determined during the last 40 minutes of the clamp.

### Measurement of GLP-1, GIP, Glucagon, and Peptide YY

Plasma levels of intact and total GLP-1 were measured on timed plasma samples before and after oral gavage with 1.25 g/kg 25% dextrose. A C-terminal radioimmunoassay for amidated GLP-1 was performed as previously described.<sup>36–38</sup> Briefly, polyclonal antiserum (code 89390) to a synthetic PG 97–107amide [GLP-1 (26–36)amide] was raised in rabbits, coupled to bovine serum albumin with carbodiimide. Antiserum 89390 has an absolute requirement for amidated C-terminus of GLP-1. Standard and I<sup>125</sup>-labeled tracer are PG 78–107amide [GLP-1 (76–36)amide] and separation of antibody-bound from free peptide was performed using plasma-coated charcoal. The total GLP-1 assay has a detection limit of 1 pmol/L and an ED<sub>50</sub> of 25 pmol/L. Intra- and interassay coefficients of variation are <6% and <15%, respectively.<sup>36,37</sup> Intact GLP-1<sup>7–36</sup> amide levels were measured on the same samples using a 2-site sandwich assay as previously described.<sup>38</sup> The intact GLP-1 (7–36)amide assay has a detection limit of 0.5 pmol/L with intra- and interassay coefficients of variation of 2% and 5%, respectively. Total PYY levels were measured on timed plasma samples before and after gavage with a solution of 25% dextrose and 20% Intralipid (1.25 g/kg and 1.5 g/kg, respectively). Intralipid was used for the postprandial PYY measurements based on the role of ingested lipid in its release.<sup>39</sup> A commercially available ELISA for rat PYY (ALPCO Diagnostics, Salem, NH) was used to measure PYY according to the manufacturer's instructions. GIP and glucagon concentrations were measured on plasma from timed pre and post-test meal samples before and after gavage with 25% dextrose/20% intralipid using a commercially available ELISA for rat GIP (Linco Research, St. Charles, MO) and an electrochemiluminescence based immunoassay for rat glucagon (n = 6/group, Meso Scale Discovery, Gaithersburg, MD).

### Statistical Analysis

Data are presented as mean ± standard error. The number of animals in each experimental group is specified in the figure legends. The statistical analysis of data from different experimental groups was performed using ANOVA followed by the Tukey-Kramer or Student-Newman Keuls posttest using Instat GraphPad 5.02 (San Diego, CA). Statistical analysis of pre and postoperative data within a group (eg, MRI and VO<sub>2</sub> data) was performed using a paired Student *t* test. Differences among groups were considered significant at *P* < 0.05.

## RESULTS

The mean body weights of the RYGB (634 ± 14 g), PF (587 ± 14 g), and AL (593 ± 14 g) groups before surgical intervention were similar, though the RYGB group was slightly heavier. Changes in body weight over time for the different experimental groups are shown in Figure 1. Compared with their presurgery weights, weight loss in the RYGB group was maximal at 84 g or 13% of total body weight POD 24 and stabilized at that level for the remainder of the 28 day study period. In contrast, the PF group only lost weight for 12 days (4.2% total body weight), then gained weight for the rest of the study, whereas the AL group gained weight continuously. During the 28 day postoperative period the AL group gained 85 ± 23 g, in comparison to the PF group which gained 19 ± 21 g, and RYGB animals which lost 78 ± 18 g (*P* < 0.001 vs. PF, AL). There were no significant differences in oxygen consumption between the groups on POD 14 (data not shown).

## Glucose Tolerance

Before surgical intervention, there were no significant differences in glucose tolerance curves between the groups (not shown in figure). To assess the effects of RYGB on glucose homeostasis, OGTTs were performed on POD 21 (Fig. 2A). Mean fasting plasma glucose levels (mg/dL) were  $92 \pm 7$  in heterozygous lean ZRs (not shown),  $191 \pm 21$  in the AL group,  $159 \pm 9$  in the PF group, and  $143 \pm 6$  in the RYGB group, ( $P < 0.05$  vs. AL). Glucose levels were elevated to a similar extent in all groups 30 minutes postgavage, but were significantly higher in the PF and AL groups at 60 and 90 minutes postgavage ( $P < 0.05$  vs. RYGB). Glucose tolerance in the RYGB animals was significantly improved as indicated by a 29% reduction in the AUC for blood glucose (Fig. 2B,  $*P < 0.05$  vs. PF, AL). On POD 21, pre-gavage insulin levels (ng/mL) were similar in the PF ( $8.6 \pm 2.5$ ) and AL ( $7.9 \pm 0.9$ ) groups, but were significantly decreased in the RYGB ( $4.2 \pm 0.7$ ,  $*P < 0.05$  vs. PF, AL) group. As shown in Figure 2C, postgavage insulin levels in the PF and AL groups remained elevated and stable over time, whereas the insulin levels in the RYGB group more than doubled at 30 minutes ( $10.7 \pm 1.9$ ), then decreased to basal levels from 60 to 120 minutes postgavage.

By POD 21, the RYGB animals demonstrate reductions in both basal insulin and glucose levels relative to PF and AL controls suggesting an improvement in insulin sensitivity. We used several mathematical models to examine the relationship between plasma glucose and insulin as an indicator of insulin sensitivity including the HOMA, QUICKI, and ISI.<sup>25,27,28</sup> On POD 21 the RYGB group demonstrated significant improvement in insulin sensitivity compared with PF and AL animals as indicated by the improvement in ISI (Fig. 2D), HOMA, and QUICKI (Table 1).

## Hyperinsulinemic, Euglycemic Clamp

The hyperinsulinemic, euglycemic clamp is commonly viewed as the “gold standard” for assessing in vivo insulin action. With this technique, insulin is administered to rapidly raise the insulin concentration while glucose is infused to maintain euglycemia. Basal glucose concentrations were highest in the AL group, intermediate in the PF group, and lowest in the RYGB group (Fig. 3A). Steady-state glucose concentrations achieved during the clamp were not different between the groups (Fig. 3C). Plasma insulin concentrations were not determined because previous studies had shown the insulin infusion rate in the current study achieves circulating levels of insulin that maximally stimulate glucose uptake by peripheral tissue (eg, skeletal muscle) and completely suppress hepatic gluconeogenesis.<sup>33–35</sup> The basal glucose turnover rates (Fig. 3B) were similar between the groups. However, insulin stimulated glucose disposal (mg/min/kg) was 2-fold greater in the RYGB group compared with either the PF or AL control groups (Fig. 3D).

## Measurement of Visceral and Subcutaneous Fat

Because changes in total body weight are not necessarily indicative of changes in body composition, we examined changes in visceral and subcutaneous fat depots over time in a cohort of animals using MRI. The cross-sectional area of subcutaneous and visceral fat for each animal was determined before surgery, normalized to 1, and then compared with values from the same rats 28 days later. Representative MRIs from each group are shown in Figure 4A. The POD 28 visceral fat in the RYGB group was essentially unchanged (3% decrease) from preoperative values (Fig. 4B) whereas the subcutaneous fat was decreased by 13% (Fig. 4C). The POD 28 visceral fat increased approximately 13% in the PF and 31% in the AL group (Fig. 4B), whereas the subcutaneous fat increased only 5% in the PF and 11% in the AL groups (Fig. 4C).

## Measurement of GLP-1, GIP, Glucagon, and PYY

The dramatic postgavage increase in plasma insulin levels observed in the RYGB animals prompted investigation into the effect of RYGB on plasma incretin levels. Fasting total GLP-1 levels were similar in the AL, PF, and RYGB groups (Fig. 5A). However, after dextrose gavage, the changes in plasma GLP-1 over time differed between the groups. Plasma GLP-1 levels remained between 35 and 22 pmol/L in the PF and AL groups from 30 to 120 minutes after gavage. In contrast, the 30 minutes postgavage total GLP-1 level increased 2-fold in the RYGB group (\**P* < 0.05 vs. PF, AL) and gradually decreased over time. Levels of intact, biologically active GLP-1 7–36 amide were measured on the same samples (Fig. 5B). Fasting and 30 to 60 minutes postgavage GLP-1 7–36 amide levels were elevated in the RYGB group (\**P* < 0.05 vs. PF, AL).

We also examined fasting and postgavage total GIP levels in the different groups (Fig. 5C). Fasting total GIP were not different between the AL, PF, and RYGB groups. However, postprandial GIP levels increased 5- to 9-fold from 30 to 60 minutes after gavage with the glucose/intralipid mixture. Although the rate of postprandial increase in GIP was more rapid in the RYGB group, there were no significant differences in plasma GIP concentrations between the groups over time. The fasting glucagon levels were also similar between the groups (*n* = 6/group; AL 202 ± 52 pg/mL; PF 186 ± 9 pg/mL; RYGB 199 ± 22 pg/mL). Postprandial plasma glucagon levels (30 to 120 minutes) were similar to fasting in the PF and AL groups. However, plasma glucagon levels increased from 199 ± 22 pg/mL to \*247 ± 10 pg/mL at 30 minutes after the test meal (\**P* < 0.05 vs. fasting), then decreased to baseline in the RYGB group (data not shown). To determine whether RYGB altered the secretion of other gut-derived peptides we measured fasting and postprandial levels of PYY after gavage with the glucose/intralipid mixture (Fig. 5D). The fasting concentration of PYY was also not different between the RYGB, PF, and AL groups. Plasma levels of PYY were essentially unchanged for 120 minutes after gavage in the PF and AL groups. In contrast, a 2-fold increase in PYY was noted in the RYGB group 30 minutes after gavage (\**P* < 0.01 vs. PF, AL), and remained elevated for the duration of the 120 minutes study period.

## DISCUSSION

The genetically obese Zucker rat develops much of the pathophysiology observed in morbidly obese patients including: progressive insulin resistance, glucose intolerance, hyperlipidemia, and hypertension.<sup>10,11,40</sup> Gastric bypass in the obese Zucker rat was first described in 1984, but was not used to investigate mechanisms of weight loss until 2002.<sup>24,41</sup> Although the Zucker rat is commonly used to study insulin resistance and T2DM, this is the first study examining the effects of RYGB on glucose homeostasis in this model. In patients, the RYGB procedure bypasses >95% of the distal stomach and the proximal jejunum resulting in bypass of the “foregut” and enhanced delivery of undigested nutrients to the ileum. Weight loss after RYGB is commonly ascribed to mechanical restriction of food intake, some degree of malabsorption, and “dumping syndrome” caused by ingestion of concentrated sweets.<sup>42</sup> Several anatomic factors limit the restrictive nature of the RYGB procedure in the Zucker rat including the thin walled gastric rumen which is unsuitable for stapling and the location of gastroesophageal junction along the lesser curvature of the stomach. Because of these anatomic factors a 20% gastric pouch with a divided RYGB was used in the current study as problems with staple line disruption were reported when a nondivided RYGB was performed.<sup>24</sup> Using this technique the RYGB group sustained significant weight loss compared with the PF and AL groups during the 28 day study period, albeit less than the 30% reduction in total body weight commonly reported after RYGB in humans. Because POD 14 VO<sub>2</sub> was similar between the groups, differences in weight loss between the PF and RYGB groups were probably not caused by differences in energy expenditure. The effects of surgery on nutrient absorption were not

examined in the current study, but represent a potential cause for differences in weight loss between the PF and RYGB groups.

The relative impact of RYGB compared with pair-feeding on glucose homeostasis was examined by comparing POD 21 OGTTs. The OGTT is commonly used to test for prediabetes or T2DM and determines how quickly glucose is cleared from the blood after a standard glucose load. Using the 1999 World Health Organization and 2004 Expert Committee criteria: fasting plasma glucose levels  $>100$  mg/dL denote impaired fasting glycemia and glucose  $>200$  mg/dL at 120 minutes confirm the diagnosis of T2DM.<sup>43</sup> Based on these criteria, all 3 groups demonstrate impaired fasting glycemia and the 120 minutes plasma glucose data indicate T2DM in both the PF and AL groups, whereas the RYGB group has improved to glucose intolerant. Although post-RYGB glucose tolerance is significantly improved relative to obese Zucker controls, it remains somewhat impaired relative to unoperated lean heterozygous Zucker controls (data not shown). Changes in glucose tolerance are noted at 6 to 7 weeks of age in the obese Zucker rat model and worsen over time.<sup>10</sup> Consequently, the finding that post-RYGB animals demonstrate some evidence of glucose intolerance on POD 21 is not surprising. The severity and duration of T2DM, as well as the magnitude of postoperative weight loss seem to be predictive of T2DM resolution after RYGB in morbidly obese patients.<sup>44</sup> Therefore, the timing of surgical intervention (10–12 weeks) may have impacted the responsiveness of glucose homeostasis in the current study. Nonetheless, the observation that glucose tolerance remained similar in PF and AL controls suggests decreased nutrient intake alone does not explain the early improvement in glucose homeostasis after RYGB.

Circulating glucose represents a critical nutrient for many tissues. The plasma glucose concentration represents the equilibrium of multiple metabolic processes including: dietary intake and absorption, glucose production (via gluconeogenesis and glycogenolysis), and glucose utilization. During the fasted state the glucose concentration is determined primarily by hepatic glucose output and glucose utilization by peripheral tissues. The postprandial increase in plasma glucose triggers insulin release from pancreatic  $\beta$ -cells by stimulating fusion of insulin-containing vesicles with the plasma membrane. Circulating insulin acts to reduce hepatic glucose production and increase peripheral GLUT4-mediated glucose uptake by striated muscle and adipose tissue. Muscle represents the principal site of insulin-stimulated glucose transport in vivo accounting for more than 75% of peripheral glucose uptake.<sup>14,45</sup> However, post-prandial hyperglycemia also increases glucose uptake by essentially all tissues via noninsulin glucose uptake which is independent of GLUT4 and mediated by mass action effect of the substrate. In the obese Zucker rat, peripheral insulin resistance is because of defective insulin signaling, reductions in the insulin-sensitive GLUT4 expression, and impaired insulin-stimulated GLUT4 membrane translocation.<sup>13,14</sup>

The release of nonesterified fatty acids and adipokines from adipose tissue is hypothesized to result in decreased responsiveness of peripheral tissues (muscle, liver, adipose) to insulin, a condition referred to as insulin resistance.<sup>45</sup> The physiologic response to obesity-related insulin resistance initially involves a compensatory increase in pancreatic  $\beta$ -cell mass and insulin secretion in the obese Zucker rat.<sup>46</sup> Consequently, an assessment of circulating insulin is important in the interpretation of the change in plasma glucose levels during the OGTT. The reduction in fasting insulin observed in the RYGB animals relative to PF and AL controls suggests an improvement in insulin sensitivity as a mechanism for post-RYGB glucose homeostasis. However, these models do not indicate whether this improvement in insulin action occurs at the level of the liver or peripheral tissues. To this end, we used the euglycemic, hyperinsulinemic clamp to directly assess peripheral (mainly skeletal muscle) glucose uptake under maximally insulin stimulating conditions. Our data clearly indicate that RYGB improves the ability of insulin to increase peripheral glucose uptake and this improvement can not be attributed to the reduction in food intake.



The distribution of body fat between the subcutaneous and visceral depots is an important determinant of insulin action. The relative abundance of visceral fat in particular correlates with insulin resistance and surgical removal of visceral fat has been shown to improve insulin sensitivity.<sup>22,47</sup> Therefore, serial MRI scans were performed in a subgroup of animals to determine whether RYGB or decreased nutrient intake preferentially affects either the subcutaneous or visceral fat depots. After RYGB, a 13% reduction in subcutaneous fat was seen with only a 3% reduction in visceral fat. The reduction in subcutaneous fat after RYGB appeared independent of food intake, whereas the post-RYGB decrease in visceral fat was largely because of decreased food intake. This finding is consistent with data from Xu et al in the Zucker rat model where reductions in retroperitoneal and epididymal fat depots after RYGB were primarily related to decreased nutrient intake.<sup>24</sup> Collectively these results provide evidence that reductions in the relative abundance of visceral fat do not explain the observed improvements in insulin action and glucose tolerance after RYGB in the Zucker rat model.

An important limitation of the current study is the lack of data on the effects of RYGB on the synthesis and/or secretion of hormones and metabolites from adipose tissue which could potentially influence insulin sensitivity. The release of inflammatory cytokines (eg, TNF, IL-6, MCP-1) from adipocytes and macrophages in visceral fat has been implicated in the pathogenesis of T2DM.<sup>48</sup> Likewise, the synthesis and secretion of metabolically active proteins or adipokines (eg, resistin, leptin, visfatin) by adipose tissue represents a potential mechanism for obesity-related insulin resistance that is not addressed by our results.<sup>47,49</sup> Consequently, the effects of RYGB on cytokine/adipokine synthesis by adipose tissue represents an important area for future study as a potential contributory mechanism for post-RYGB glucose homeostasis.

Despite this caveat, the observed changes in postprandial gut peptide production provide evidence that alterations in incretin production may contribute to improvements in glycemic control after RYGB. GIP is secreted by K cells in the duodenum and jejunum in response to ingested fat and glucose. GLP-1, a product of the proglucagon gene is secreted by L cells of the distal ileum and colon in response to intraluminal fats and carbohydrates. GIP and GLP-1 are rapidly degraded by dipeptidyl peptidase-4 starting shortly after secretion. Differential processing of the proglucagon gene results in multiple circulating proglucagon peptides. However, only the GLP-1 7–36 amide and Gly-extended forms are bioactive and stimulate insulin release from pancreatic  $\beta$ -cells. As a result of DPP-IV degradation, <25% of newly secreted GLP-1 reaches the portal circulation as the intact, active form and only 10% to 15% reaches the systemic circulation.<sup>15</sup> This observation has raised concerns regarding the importance of portal GLP-1 concentrations in regulating glucose homeostasis and represents a potential limitation of the current study which only measured systemic incretin levels.<sup>50</sup> Normally, GIP and GLP-1 induce  $\beta$ -cell proliferation, inhibit apoptosis, and stimulate glucose-dependent  $\beta$ -cell insulin secretion via specific receptor-mediated pathways.<sup>15,16,51</sup> The simultaneous increase in plasma GLP-1 and insulin concentrations observed 30 minutes after gavage in the RYGB group suggests the insulinotropic effect of GLP-1 on pancreatic  $\beta$ -cells contributes to glycemic control. However, the relative importance of incretin-mediated insulin release versus incretin-mediated improvement in peripheral insulin sensitivity/action in post-RYGB glycemic control is difficult to ascertain because both mechanisms are likely involved. Although there do not seem to be GLP-1 receptors in either muscle or liver, extrapancreatic effects of GLP-1 on insulin-independent glucose disposal/metabolism in liver and muscle have been described.<sup>17,18</sup> More recently, GLP-1 receptors on vagal afferents in the portal vein were shown to improve glucose tolerance without altering the concentration of circulating insulin.<sup>50</sup> Consequently the increase in total and intact GLP-1 7–36 amide observed after RYGB potentially acts by multiple mechanisms to improve glucose homeostasis. The increase in total plasma GLP-1 after gavage may be because of hyperplasia of intestinal endocrine cells. Increased expression of proglucagon, proconvertase 1/3, and chromogranin genes has been

described in the transposed ileal segment after ileal transposition and supports a potential role for gut endocrine hyperplasia as a contributing factor.<sup>52</sup> Although fasting and postgavage plasma GIP concentrations were similar to controls after RYGB, the insulinotropic effects of GIP seem to be decreased in T2DM as a result of reductions in  $\beta$ -cell GIP receptors and postreceptor defects in  $\beta$ -cell GIP signaling.<sup>19,53–55</sup> Consequently, evaluating the effects of RYGB on GIP bioactivity will require a more detailed analysis of the relative abundance of GIP receptors and postreceptor signaling events in pancreatic  $\beta$ -cells. The increase in postprandial PYY observed after RYGB is consistent with changes in PYY noted after RYGB in morbidly obese patients.<sup>56,57</sup> Although PYY is a known satiety factor posited to mediate postsurgical reductions in appetite and improved satiety, there is no evidence that postgavage changes in PYY contribute directly to post-RYGB improvements in glucose homeostasis. The finding of paradoxical hyperglucagonemia after RYGB in the current study is consistent with results of Laferrere et al who observed a post-OGTT increase in glucagon 1 month after RYGB in morbidly obese patients with T2DM.<sup>58</sup>

The foregut and “hindgut” hypotheses have been proposed to explain the effects of postsurgical RYGB intestinal anatomy on insulin resistance and T2DM.<sup>7</sup> The foregut hypothesis suggests bypass of the duodenum and proximal jejunum alone improves T2DM.<sup>59</sup> The hindgut hypothesis suggests enhanced delivery of undigested nutrients to the ileum stimulates gut peptide secretion by mucosal L cells (eg, GLP-1, PYY) which act to inhibit appetite and improve glucose homeostasis. Several studies have examined fasting and postprandial gut peptides in morbidly obese patients after RYGB.<sup>57,60,61</sup> Korner et al noted an exaggerated postprandial insulin response and changes in ghrelin and PYY consistent with increased satiety as a mechanism of weight loss after RYGB.<sup>56</sup> Similar changes in postprandial glucose tolerance, insulin, GLP-1, PYY, and GIP levels were recently described as early as 1 month after RYGB in morbidly obese patients.<sup>60</sup> However, the current study is the first to characterize fasting and postprandial incretins after RYGB in the obese Zucker rat model and directly assess insulin action using the euglycemic hyperinsulinemic clamp. Although fasting levels of total GLP-1, GIP, and PYY were similar in the experimental groups, the postprandial increase in GLP-1, GIP, PYY, and insulin in the RYGB group seems to correlate with improvements in insulin sensitivity and glucose homeostasis. Importantly, the changes in glucose homeostasis and gut peptide secretion in the Zucker rat model resemble those observed in post-RYGB patients confirming its utility as an experimental model for metabolic research on obesity and T2DM.

## Acknowledgments

The authors thank Dr. Pengxiang She (Department. Cellular and Molecular Physiology, Penn State College of Medicine) for his technical assistance with indirect calorimetry studies, Dr. Timothy Mosher (Department. of Radiology) for his assistance with MRI studies examining adipose depots, Dr. Jens Holst (University of Copenhagen, Denmark) for performing total GLP-1 and GLP-1 7–36 amide assays, and Ethicon Corporation (Cincinnati, OH) for providing stapling devices.

Supported in part by National Institute of Health Grants GM-55639 (to R.N.C), GM-38032 (to C.H.L), and DK062880 (to C.L). This project is funded, in part, under grants with the Pennsylvania Department of Health using Tobacco Settlement Funds.

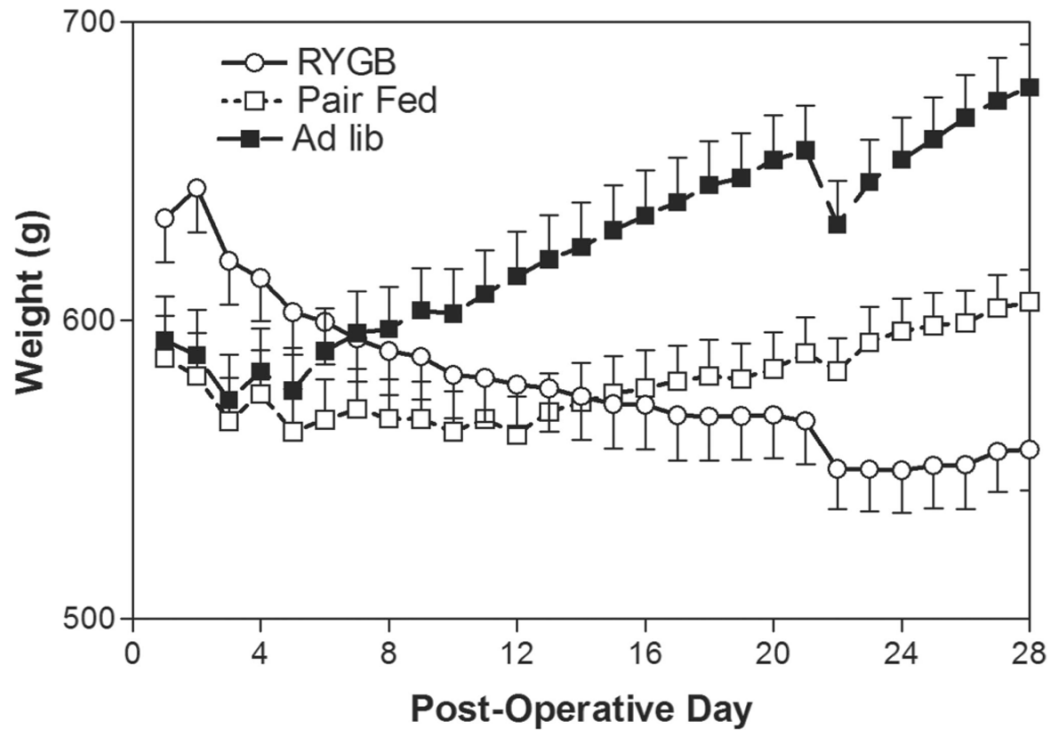
## References

1. Fontaine KR, Redden DT, Wang C, et al. Years of life lost due to obesity. *JAMA* 2003;289:187–193. [PubMed: 12517229]
2. Sjostrom L, Lindroos AK, Peltonen M, et al. Lifestyle, diabetes, and cardiovascular risk factors 10 years after bariatric surgery. *N Engl J Med* 2004;351:2683–2693. [PubMed: 15616203]
3. Pories WJ, MacDonald KG Jr, Flickinger EG, et al. Is type II diabetes mellitus (NIDDM) a surgical disease? *Ann Surg* 1992;215:633–642. [PubMed: 1632685]

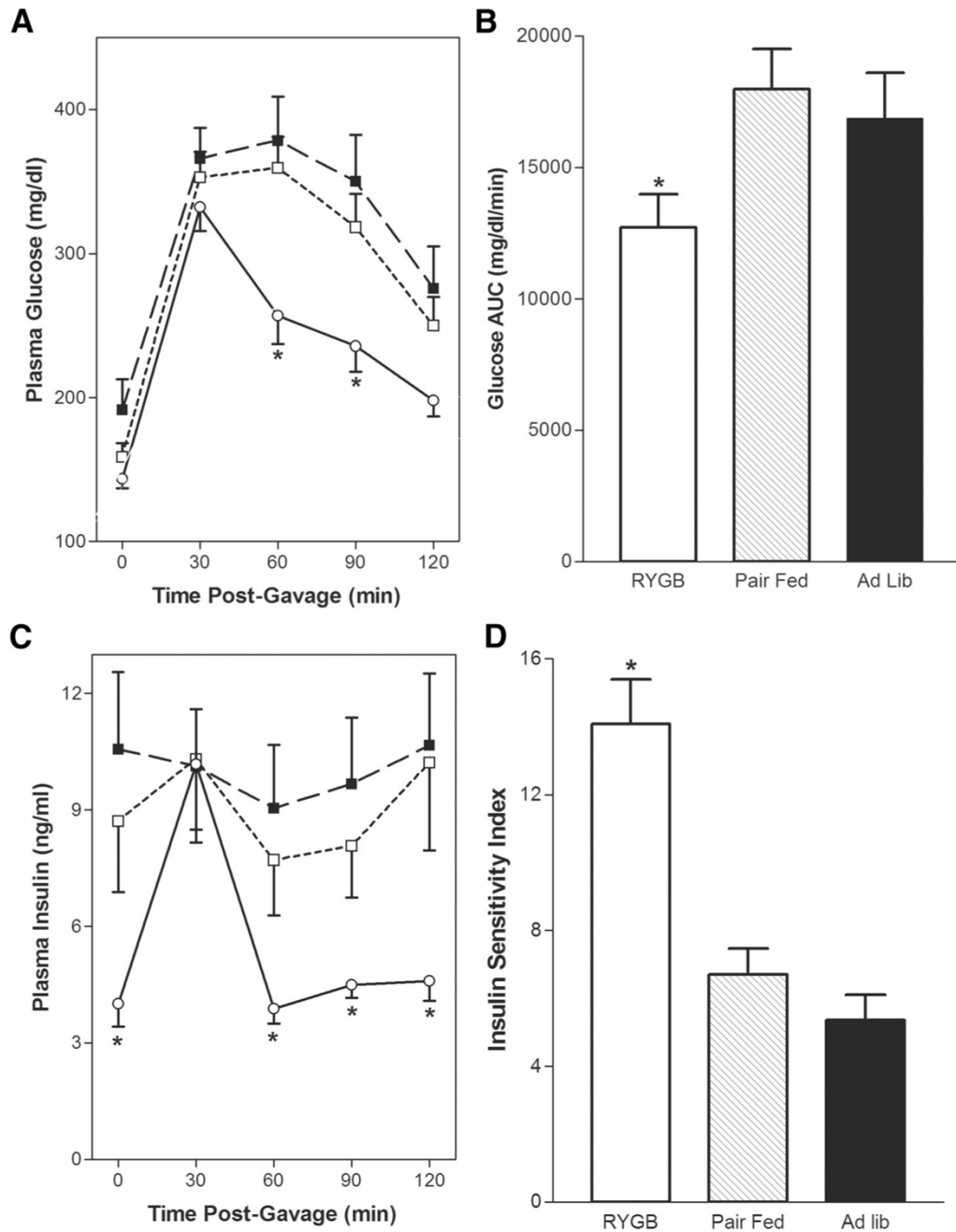
4. Pories WJ. Diabetes: the evolution of a new paradigm. *Ann Surg* 2004;239:12–13. [PubMed: 14685094]
5. Cowan GS Jr, Buffington CK. Significant changes in blood pressure, glucose, and lipids with gastric bypass surgery. *World J Surg* 1998;22:987–992. [PubMed: 9717426]
6. Rubino F, Gagner M, Gentileschi P, et al. The early effect of the Roux-en-Y gastric bypass on hormones involved in body weight regulation and glucose metabolism. *Ann Surg* 2004;240:236–242. [PubMed: 15273546]
7. Cummings DE, Overduin J, Foster-Schubert KE. Gastric bypass for obesity: mechanisms of weight loss and diabetes resolution. *J Clin Endocrinol Metab* 2004;89:2608–2615. [PubMed: 15181031]
8. Cummings DE, Overduin J, Foster-Schubert KE, et al. Role of the bypassed proximal intestine in the anti-diabetic effects of bariatric surgery. *Surg Obes Relat Dis* 2007;3:109–115. [PubMed: 17386391]
9. Zucker LM. Hereditary obesity in the rat associated with hyperlipemia. *Ann N Y Acad Sci* 1965;131:447–458. [PubMed: 5216982]
10. Ionescu E, Sauter JF, Jeanrenaud B. Abnormal oral glucose tolerance in genetically obese (fa/fa) rats. *Am J Physiol* 1985;248:E500–506. [PubMed: 3887938]
11. Kasiske BL, O'Donnell MP, Keane WF. The Zucker rat model of obesity, insulin resistance, hyperlipidemia, and renal injury. *Hypertension* 1992;19:1110–115. [PubMed: 1730447]
12. Chen D, Wang MW. Development and application of rodent models for type 2 diabetes. *Diabetes Obes Metab* 2005;7:307–317. [PubMed: 15955116]
13. Chang L, Chiang SH, Saltiel AR. Insulin signaling and the regulation of glucose transport. *Mol Med* 2004;10:65–71. [PubMed: 16307172]
14. Shepherd PR, Kahn BB. Glucose transporters and insulin action—implications for insulin resistance and diabetes mellitus. *N Engl J Med* 1999;341:248–257. [PubMed: 10413738]
15. Baggio LL, Drucker DJ. Biology of incretins: GLP-1 and GIP. *Gastroenterology* 2007;132:2131–2157. [PubMed: 17498508]
16. Drucker DJ. The role of gut hormones in glucose homeostasis. *J Clin Invest* 2007;117:24–32. [PubMed: 17200703]
17. Redondo A, Trigo MV, Acitores A, et al. Cell signalling of the GLP-1 action in rat liver. *Mol Cell Endocrinol* 2003;204:43–50. [PubMed: 12850280]
18. Valverde I, Villanueva-Penacarrillo ML, Malaisse WJ. Pancreatic and extrapancreatic effects of GLP-1. *Diabetes Metab* 2002;28:3S85–89. [PubMed: 12688638]
19. Lynn FC, Pamir N, Ng EH, et al. Defective glucose-dependent insulinotropic polypeptide receptor expression in diabetic fatty Zucker rats. *Diabetes* 2001;50:1004–1011. [PubMed: 11334402]
20. Holst JJ, Gromada J. Role of incretin hormones in the regulation of insulin secretion in diabetic and nondiabetic humans. *Am J Physiol Endocrinol Metab* 2004;287:E199–206. [PubMed: 15271645]
21. Kershaw EE, Flier JS. Adipose tissue as an endocrine organ. *J Clin Endocrinol Metab* 2004;89:2548–2556. [PubMed: 15181022]
22. Gabriely I, Ma XH, Yang XM, et al. Removal of visceral fat prevents insulin resistance and glucose intolerance of aging: an adipokine-mediated process? *Diabetes* 2002;51:2951–2958. [PubMed: 12351432]
23. Hotamisligil GS, Shargill NS, Spiegelman BM. Adipose expression of tumor necrosis factor- $\alpha$ : direct role in obesity-linked insulin resistance. *Science* 1993;259:87–91. [PubMed: 7678183]
24. Xu Y, Ohinata K, Meguid MM, et al. Gastric bypass model in the obese rat to study metabolic mechanisms of weight loss. *J Surg Res* 2002;107:56–63. [PubMed: 12384065]
25. McIntyre N, Holdsworth CD, Turner DS. New interpretation of oral glucose tolerance. *Lancet* 1964;2:20–21. [PubMed: 14149200]
26. Turner RC, Holman RR, Matthews D, et al. Insulin deficiency and insulin resistance interaction in diabetes: estimation of their relative contribution by feedback analysis from basal plasma insulin and glucose concentrations. *Metabolism* 1979;28:1086–1096. [PubMed: 386029]
27. Chen H, Sullivan G, Yue LQ, et al. QUICKI is a useful index of insulin sensitivity in subjects with hypertension. *Am J Physiol Endocrinol Metab* 2003;284:E804–812. [PubMed: 12678026]

28. Matsuda M, DeFronzo RA. Insulin sensitivity indices obtained from oral glucose tolerance testing: comparison with the euglycemic insulin clamp. *Diabetes Care* 1999;22:1462–1470. [PubMed: 10480510]
29. Barac-Nieto M, Gupta RK. Use of proton MR spectroscopy and MR imaging to assess obesity. *J Magn Reson Imaging* 1996;6:235–238. [PubMed: 8851434]
30. Calderan L, Marzola P, Nicolato E, et al. In vivo phenotyping of the ob/ob mouse by magnetic resonance imaging and 1H-magnetic resonance spectroscopy. *Obesity (Silver Spring)* 2006;14:405–414. [PubMed: 16648611]
31. She P, Reid TM, Bronson SK, et al. Disruption of BCATm in mice leads to increased energy expenditure associated with the activation of a futile protein turnover cycle. *Cell Metab* 2007;6:181–194. [PubMed: 17767905]
32. Crist GH, Xu B, Lanoue KF, et al. Tissue-specific effects of in vivo adenosine receptor blockade on glucose uptake in Zucker rats. *FASEB J* 1998;12:1301–1308. [PubMed: 9761773]
33. Lang CH. Sepsis-induced insulin resistance in rats is mediated by a beta-adrenergic mechanism. *Am J Physiol* 1992;263:E703–711. [PubMed: 1329550]
34. Lang CH, Dobrescu C, Bagby GJ. Tumor necrosis factor impairs insulin action on peripheral glucose disposal and hepatic glucose output. *Endocrinology* 1992;130:43–52. [PubMed: 1727716]
35. Lang CH, Dobrescu C, Meszaros K. Insulin-mediated glucose uptake by individual tissues during sepsis. *Metabolism* 1990;39:1096–1107. [PubMed: 2215256]
36. Hvidberg A, Nielsen MT, Hilsted J, et al. Effect of glucagon-like peptide-1 (proglucagon 78–107amide) on hepatic glucose production in healthy man. *Metabolism* 1994;43:104–108. [PubMed: 8289665]
37. Orskov C, Rabenhøj L, Wettergren A, et al. Tissue and plasma concentrations of amidated and glycine-extended glucagon-like peptide I in humans. *Diabetes* 1994;43:535–539. [PubMed: 8138058]
38. Wilken MLF, Buckley D, Holst JJ. New highly specific immunoassays for glucagon-like peptide-1 (GLP-1). *Diabetologia* 1999;(suppl 1):A196.
39. Strader AD, Vahl TP, Jandacek RJ, et al. Weight loss through ileal transposition is accompanied by increased ileal hormone secretion and synthesis in rats. *Am J Physiol Endocrinol Metab* 2005;288:E447–453. [PubMed: 15454396]
40. Fissoune R, Pellet N, Chaabane L, et al. Evaluation of adipose tissue distribution in obese fa/fa Zucker rats by in vivo MR imaging: effects of peroxisome proliferator-activated receptor agonists. *Magma* 2004;17:229–235. [PubMed: 15624103]
41. Young EA, Taylor MM, Taylor MK, et al. Gastric stapling for morbid obesity: gastrointestinal response in a rat model. *Am J Clin Nutr* 1984;40:293–302. [PubMed: 6205581]
42. Mallory GN, Macgregor AM, Rand CS. The influence of dumping on weight loss after gastric restrictive surgery for morbid obesity. *Obes Surg* 1996;6:474–478. [PubMed: 10729895]
43. Diagnosis and classification of diabetes mellitus. *Diabetes Care* 2004;27(suppl 1):S5–10. [PubMed: 14693921]
44. Schauer PR, Burguera B, Ikramuddin S, et al. Effect of laparoscopic Roux-en Y gastric bypass on type 2 diabetes mellitus. *Ann Surg* 2003;238:467–484. [PubMed: 14530719]discussion 484–465
45. Kahn SE, Hull RL, Utzschneider KM. Mechanisms linking obesity to insulin resistance and type 2 diabetes. *Nature* 2006;444:840–846. [PubMed: 17167471]
46. Jetton TL, Lausier J, LaRock K, et al. Mechanisms of compensatory beta-cell growth in insulin-resistant rats: roles of Akt kinase. *Diabetes* 2005;54:2294–2304. [PubMed: 16046294]
47. Hansen E, Hajri T, Abumrad NN. Is all fat the same? The role of fat in the pathogenesis of the metabolic syndrome and type 2 diabetes mellitus. *Surgery* 2006;139:711–716. [PubMed: 16782424]
48. Rosen ED, Spiegelman BM. Adipocytes as regulators of energy balance and glucose homeostasis. *Nature* 2006;444:847–853. [PubMed: 17167472]
49. Fontana L, Eagon JC, Trujillo ME, et al. Visceral fat adipokine secretion is associated with systemic inflammation in obese humans. *Diabetes* 2007;56:1010–1013. [PubMed: 17287468]
50. Vahl TP, Tauchi M, Durler TS, et al. Glucagon-like peptide-1 (GLP-1) receptors expressed on nerve terminals in the portal vein mediate the effects of endogenous GLP-1 on glucose tolerance in rats. *Endocrinology* 2007;148:4965–4973. [PubMed: 17584962]

51. Murphy KG, Dhillo WS, Bloom SR. Gut peptides in the regulation of food intake and energy homeostasis. *Endocr Rev* 2006;27:719–727. [PubMed: 17077190]
52. Patriti A, Aisa MC, Annetti C, et al. How the hindgut can cure type 2 diabetes. Ileal transposition improves glucose metabolism and beta-cell function in Goto-kakizaki rats through an enhanced Proglucagon gene expression and L-cell number. *Surgery* 2007;142:74–85. [PubMed: 17630003]
53. Nauck MA, Heimesaat MM, Orskov C, et al. Preserved incretin activity of glucagon-like peptide 1 [7–36 amide] but not of synthetic human gastric inhibitory polypeptide in patients with type-2 diabetes mellitus. *J Clin Invest* 1993;91:301–307. [PubMed: 8423228]
54. Vilsboll T, Krarup T, Madsbad S, et al. Defective amplification of the late phase insulin response to glucose by GIP in obese Type II diabetic patients. *Diabetologia* 2002;45:1111–1119. [PubMed: 12189441]
55. Piteau S, Olver A, Kim SJ, et al. Reversal of islet GIP receptor down-regulation and resistance to GIP by reducing hyperglycemia in the Zucker rat. *Biochem Biophys Res Commun* 2007;362:1007–1012. [PubMed: 17803965]
56. Korner J, Inabnet W, Conwell IM, et al. Differential effects of gastric bypass and banding on circulating gut hormone and leptin levels. *Obesity (Silver Spring)* 2006;14:1553–1561. [PubMed: 17030966]
57. le Roux CW, Welbourn R, Werling M, et al. Gut hormones as mediators of appetite and weight loss after Roux-en-Y gastric bypass. *Ann Surg* 2007;246:780–785. [PubMed: 17968169]
58. Laferrere B, Teixeira J, McGinty J, et al. Effect of weight loss by gastric bypass surgery versus hypocaloric diet on glucose and incretin levels in patients with type 2 diabetes. *J Clin Endocrinol Metab* 2008;93:2479–2485. [PubMed: 18430778]
59. Rubino F, Marescaux J. Effect of duodenal-jejunal exclusion in a non-obese animal model of type 2 diabetes: a new perspective for an old disease. *Ann Surg* 2004;239:1–11. [PubMed: 14685093]
60. Laferrere B, Heshka S, Wang K, et al. Incretin levels and effect are markedly enhanced 1 month after Roux-en-Y gastric bypass surgery in obese patients with type 2 diabetes. *Diabetes Care* 2007;30:1709–1716. [PubMed: 17416796]
61. Korner J, Bessler M, Inabnet W, et al. Exaggerated glucagon-like peptide-1 and blunted glucose-dependent insulinotropic peptide secretion are associated with Roux-en-Y gastric bypass but not adjustable gastric banding. *Surg Obes Relat Dis*. 2007



**FIGURE 1.** Changes in body weight after RYGB in obese Zucker rats Daily mean body weight (g,  $\pm$  SE) for the RYGB (n = 34), PF (n = 23), and AL (n = 22) groups over the 28-day-study period.

**FIGURE 2.**

Effect of RYGB on POD 21 glucose tolerance and insulin sensitivity. A, Fasting ( $t_0$ ) and postgavage glucose levels (mg/dL) were measured 30, 60, 90, and 120 minutes after gavage with 1.25 g/kg 25% dextrose on POD 21 in the RYGB-○-(n = 24), PF-□-(n = 15), and AL-■-(n = 15) groups. B, Glucose AUC was calculated as described in Methods for each of the experimental groups. C, Plasma insulin levels (ng/mL) were measured before ( $t_0$ ), 30, 60, 90, and 120 minutes after dextrose gavage on POD 21 in the RYGB-○-(n = 24), PF-□-(n = 15), and AL-■-(n = 15) groups. D, Insulin sensitivity index was calculated as described in Methods for each of the glucose tolerance curves in panels A and C. Data are mean  $\pm$  SE, \* $P$  < 0.05 versus PF and AL for all panels.

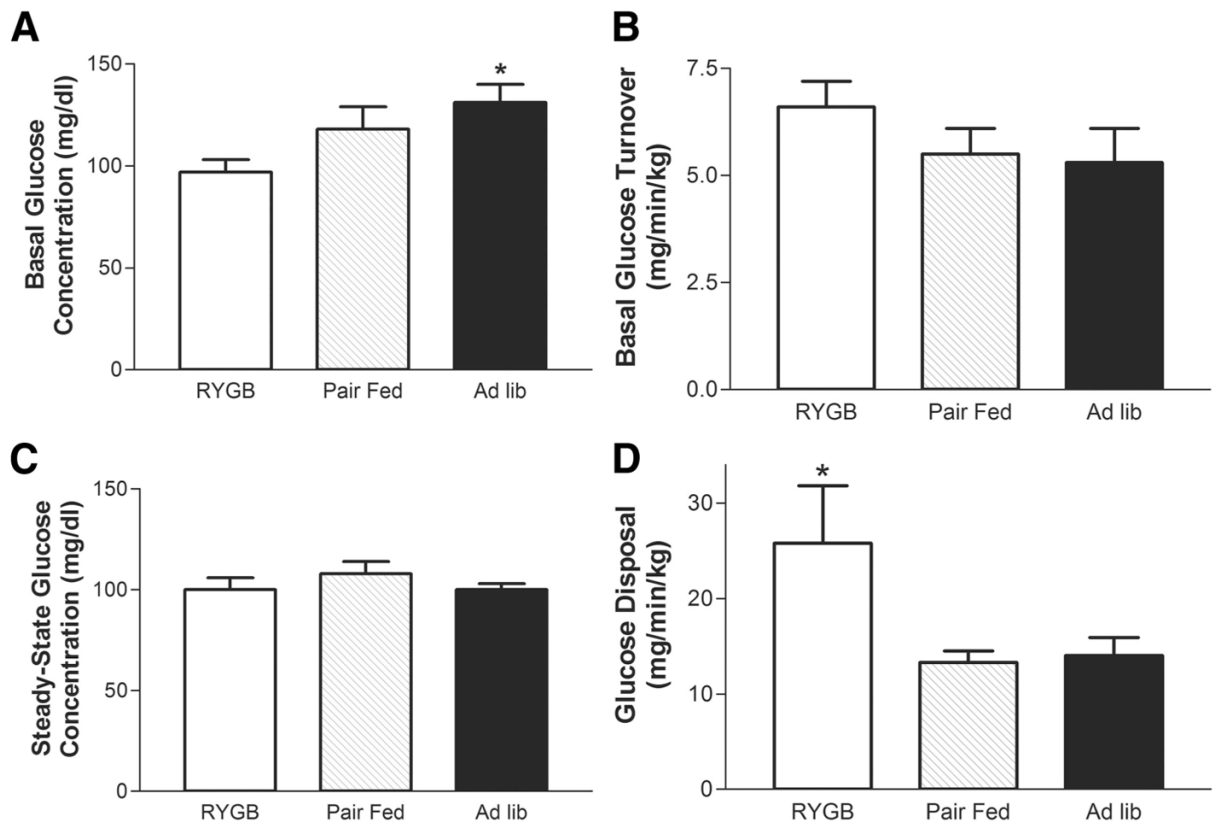


**FIGURE 3.**

Euglycemic, hyperinsulinemic insulin clamp. Panels A, and C, Basal and steady-state plasma glucose concentrations were determined before and during the clamp procedure, respectively, as described in Methods for the AL ( $n = 5$ ), PF ( $n = 4$ ), and RYGB ( $n = 4$ ) groups on POD 21. Panels B, and D, Basal glucose turnover (mg/min/kg) was determined before the start of the clamp using a constant infusion of  $^3\text{H}$ -glucose. Whole body glucose disposal (mg/min/kg) was determined during the last 1 hour of the clamp and represents the average glucose infusion rate during this time frame. Data are mean  $\pm$  SE, \* $P < 0.05$  RYGP versus PF and AL for all panels.



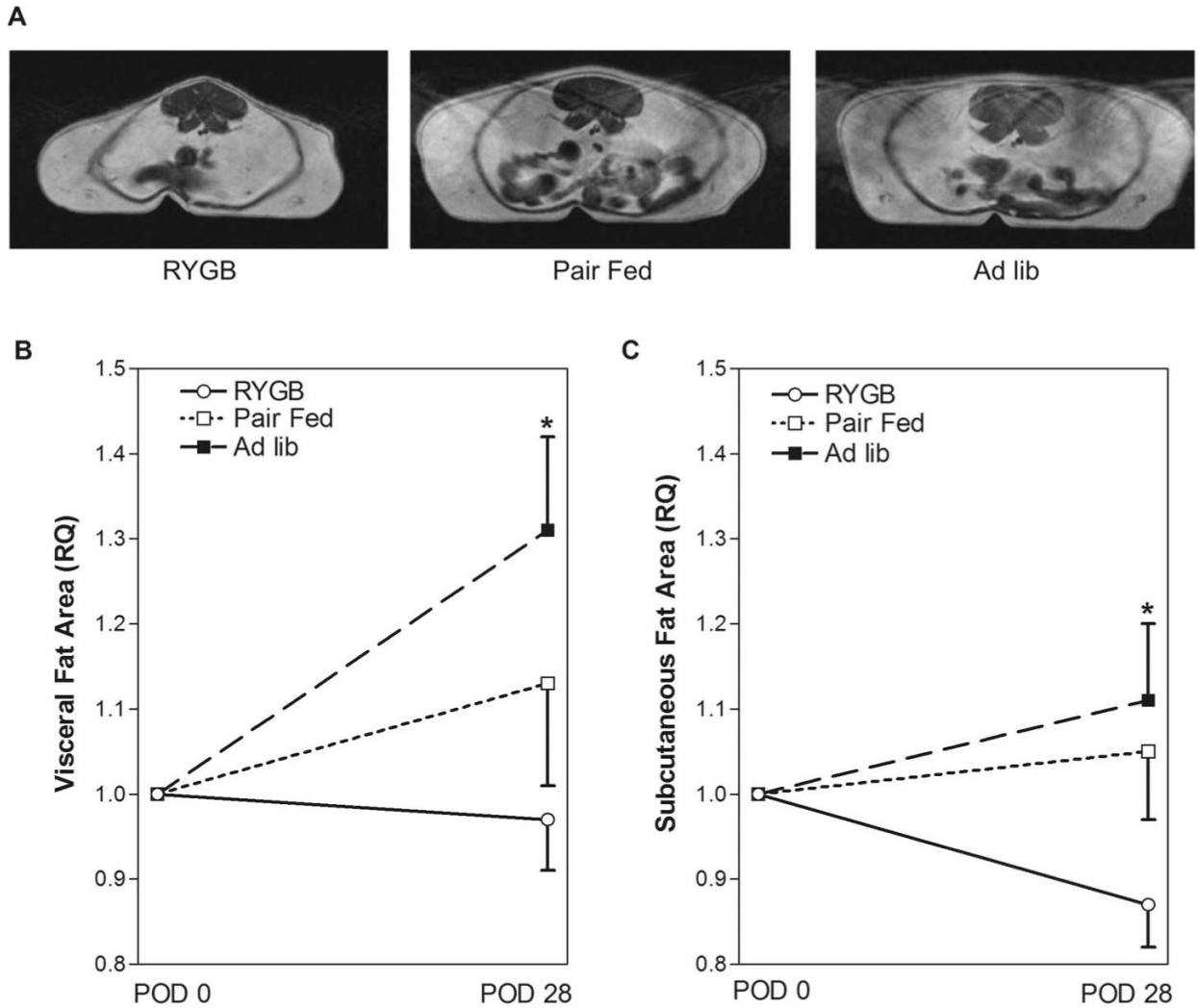


**FIGURE 4.**

Visceral and subcutaneous fat depots after RYGB in the obese Zucker rat. **A**, Representative MRI scans from obese Zucker rats in the RYGB, PF, and Ad lib groups. **B**, Effects of RYGP on visceral fat depot. The relative abundance of visceral fat in the RYGB (n = 11), PF (n = 8), and AL (n = 8) groups was determined using MRI before surgery and on POD 28 as described in Methods. **C**, Effects of RYGP on subcutaneous fat depot. The relative abundance of subcutaneous fat in the RYGB (n = 11), PF (n = 8), and AL (n = 8) groups was determined using MRI before surgery and on POD 28 as described in Methods. Data are mean ± SE, \*P < 0.05 RYGP versus AL for all panels.

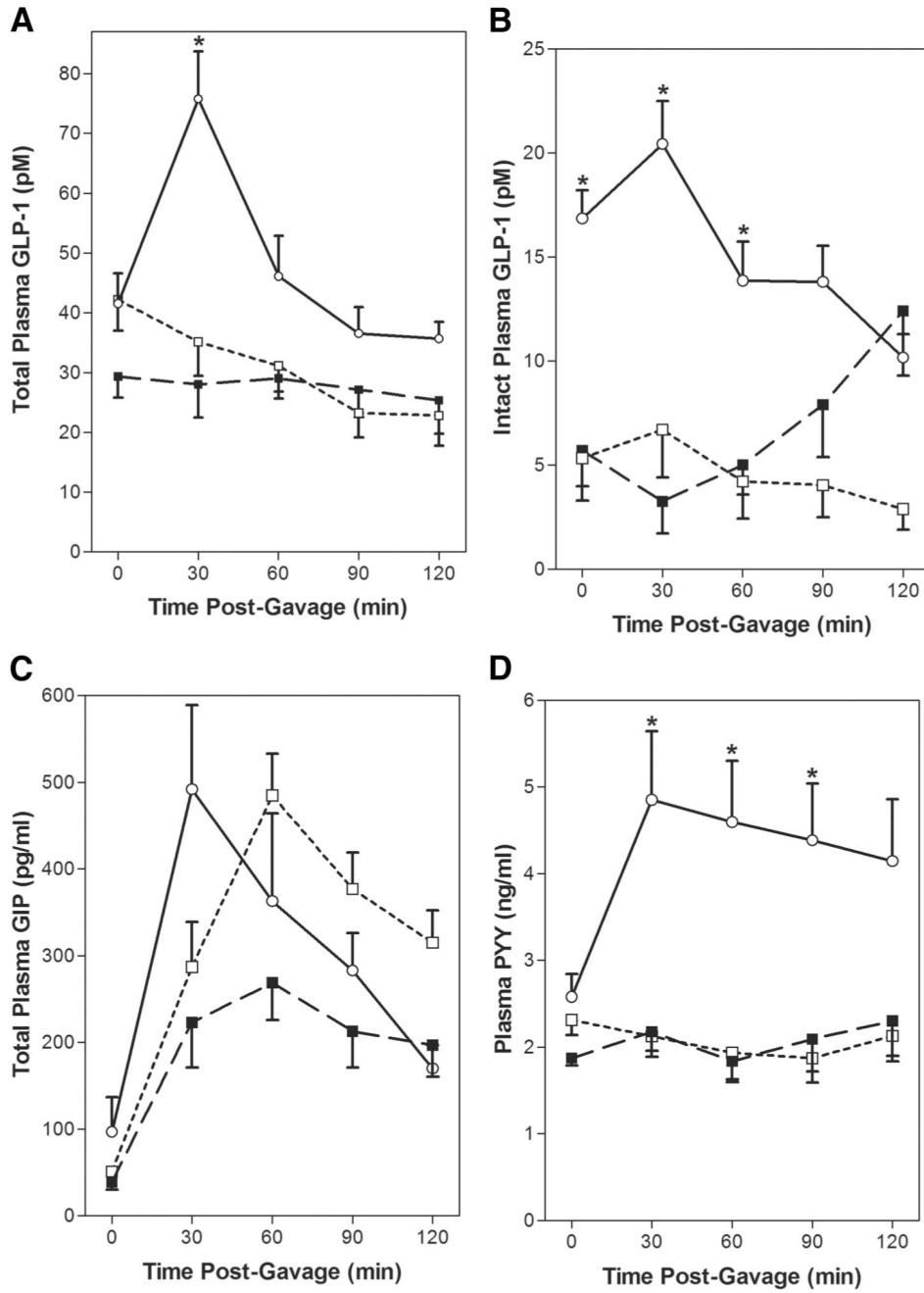


**FIGURE 5.** RYGB alters postprandial gut peptide secretion. Fasting ( $t_0$ ) and postgavage plasma samples were collected at 30, 60, 90, and 120 minutes after gavage on POD 21 as described in Methods. Data are mean  $\pm$  SE, \* $P < 0.05$  RYGB versus PF and AL for all panels. A, Total GLP-1 and B, Intact GLP-1 are in pM, RYGB-○-( $n = 9$ ), PF-□-( $n = 9$ ), and AL-■-( $n = 9$ ). Total GIP C, is reported in pg/mL, and PYY D, is reported in ng/mL, RYGB-○ - ( $n = 11$ ), PF-□-( $n = 8$ ), and AL-■-( $n = 8$ ).

**TABLE 1**

Effects of RYGB on Glucose Tolerance and Insulin Sensitivity

| Group    | POD21 Weight Change (g) | POD21 Glu AUC | POD21 HOMA  | POD21 QUICKI   |
|----------|-------------------------|---------------|-------------|----------------|
| GBP (24) | -94 ± 18*               | 12728 ± 1252* | 38.6 ± 6.5* | 0.245 ± 0.003* |
| PF (15)  | 75 ± 21                 | 17980 ± 1526  | 92.9 ± 18   | 0.223 ± 0.002  |
| AL (14)  | 130 ± 23                | 16868 ± 1742  | 136.5 ± 28  | 0.216 ± 0.004  |

The effects of RYGB on body weight, area under the curve of the OGTT (Glu AUC), and calculated insulin sensitivity (HOMA, QUICKI) are shown. Values are means ± SE; n = 24, 15, and 14, respectively.

\*  $P < 0.05$  compared with PF, AL.